Performance analysis of two-dimensional photonic crystal octagonal ring resonator based eight channel demultiplexer

Venkatachalam Kannaiyan[1, 2*], Sriram Kumar Dhamodharan[1],
Robinson Savarimuthu[1, 2]

[1]Department of Electronics and Communication Engineering, National Institute of Technology,
 Tiruchirappalli, Tamil Nadu, India

[2]Mount Zion College of Engineering and Technology, Pudukkottai, Tamil Nadu, India

*Corresponding author: venkatachalamece@gmail.com

We proposed a high performance eight channel demultiplexer using two-dimensional photonic crystal octagonal ring resonator for wavelength division multiplexing applications. The performance parameters such as transmission efficiency, Q factor, spectral width, resonant wavelength, crosstalk and channel spacing of the proposed demultiplexers are evaluated. The plane wave expansion method manipulates photonic band gap of periodic and non-periodic structure. Finite-difference time-domain method is used to evaluate the performance parameters of designed two-dimensional photonic crystal structure. The proposed demultiplexer provides overall transmission efficiency, Q factor, spectral width of about 98%, 1968 and 0.8 nm, respectively. The ultra-compact eight channel demultiplexer performs better than the reported one. Hence this work can be implemented for real time applications.

Keywords: two-dimensional photonic crystal, photonic band gap, ring resonator, waveguide, demultiplexer, wavelength division multiplexing.

1. Introduction

Nowadays the design of high performance with miniaturized optical devices is one of the most important technological challenges of information processing systems in optical communication. Photonic crystal (PC) is one of the right candidates for wavelength division multiplexing (WDM) systems as it offers highly wavelength sensitive, terahertz speed and miniaturized size without degrading the performance of the device. Recently, WDM [1] systems receive keen attention in research community as it supports a big number of channels with narrow channel spacing in a single fibre. It is classified by coarse wavelength division multiplexing (CWDM) and dense wavelength division multiplexing (DWDM). The CWDM system (ITU-T Recommendation G.694.2) is

supporting a smaller number of channels over the wavelength range between 1260 and 1675 nm with 20 nm channel spacing. Alternatively, the DWDM system (ITU-T Recommendation G.694.1) is facilitating a bigger number of channels from 1535 to 1565 nm with narrow channel spacing (1.6 nm/0.8 nm/0.4 nm). Hence, DWDM system will be employed for point-to-point high capacity network; however, CWDM will be used for access networks and regional networks. In this work, DWDM system is considered for demultiplexer design.

Typically, PC based optical devices are realized either in cubic lattice or in hexagonal lattice. The cubic is referred to as a square lattice and hexagonal is referred to as a triangular lattice. In the cubic lattice, photonic band gap (PBG) size is narrow [2], there is low dispersion, high power transmission [3], and easy fabrication facility compared to the hexagonal lattice. Hence, the proposed device is designed using two-dimensional photonic crystal (2DPC) in a cubic lattice. The cubic lattice is composed of the periodic array of dielectric rods which are embedded in an air medium. The 2DPC is having PBG as the PC is composed of periodic dielectric constant variations in two different directions. The design of PBG [4] in PC is an active role to identify the desired operating range. It is used to control and manipulate the light waves propagating through PC. The lattice constant a, radius of dielectric rod r and refractive index difference Δ are the important PC parameters to generate and control PBG. The device can be realized by various defects that are introduced in PC. The defects are classified as line defects and point defects. Once defects are introduced in the periodic structure, the PBG is entirely broken, which in turn makes the modes propagate inside the defect based structure. The defects are used to trap or localize the light. By having the aforementioned principle, many PC based optical devices are realized, such as cavity, ring resonator (RR), waveguide, *etc*., which are actively used to design optical filter [5–13], switches [14], sensors [15], polarizers [16], mirrors [17], splitters [18], multiplexers [19], and demultiplexers [20–35], *etc*.

In the literature survey, the PC based demultiplexers are designed by introducing point defects and line defects alone or combining point and line defects. Generally, the combination of point and line defects is used to develop ring resonator based PC devices. The demultiplexers are designed using different shapes using either line or point defects alone, such as *Y* shape [20], *T* shape [23], cascaded *T* shape [24], tree shape [32] which offer better transmission efficiency, high quality factor, narrow channel spacing and small size. However, it is very difficult to reduce crosstalk. Alternatively, the eight shaped ring resonator [21, 31], elliptical type ring resonator [22, 33], ring resonator based square ring resonator [25–29], circle type ring resonator [30] and square ring resonator based octagon shaped resonator [34] are incorporated to design the demultiplexer. The ring resonator based demultiplexer facilitates high transmission efficiency, medium level of *Q* factor, channel spacing and low crosstalk which is considered in this attempt. In this paper, a ring resonator based octagonal cavity eight channel demultiplexer is proposed and designed for WDM applications. The performance

parameters, namely transmission efficiency, *Q* factor, channel spacing, resonant wavelength and spectral width are investigated.

The remaining part of this paper is organised as follows. In Section 2, the numerical methods which are required to accord PBG and output spectrum are discussed. The PBG in 2DPC structure is demonstrated in Section 3. The proposed photonic crystal ring resonator (PCRR) based eight channel demultiplexer is presented in Section 4. The output response and its significance is described in Section 5. Finally, Section 6 conclude the paper.

2. Numerical analysis

Several numerical methods are reported to obtain PBG and normalized output spectra of the periodic and non-periodic PC structure. They are plane wave expansion (PWE) method [36], transfer matrix method (TMM) [37], finite-difference time-domain method (FDTD) [38], and finite element method (FEM) [39], *etc*. The PWE and FDTD methods are predicting the accurate behaviour of 2DPC. Hence, the PWE is applied in the frequency domain to analyse the PBG and estimates the electromagnetic modes in PC structures. The band diagram calculations of electric field are carried out by solving Maxwell's equation [4] which is

$$\nabla \times E + \frac{\partial B}{\partial t} = 0 \tag{1}$$

$$\nabla \cdot B = 0 \tag{2}$$

$$\nabla \times H - \frac{\partial D}{\partial t} = J \tag{3}$$

$$\nabla \cdot D = \rho \tag{4}$$

The magnetic field $H(r)$ equation is

$$\nabla \times \left[\frac{1}{\varepsilon(r)} \nabla \times H(r) \right] = \left(\frac{\omega}{c} \right)^2 H(r) \tag{5}$$

The Maxwell electromagnetism appears as an eigenvalue problem for the harmonic modes of the magnetic field $H(r)$, and the solution of electric field is

$$\nabla \times \nabla \times E(r) = \left(\frac{\omega}{c} \right)^2 \varepsilon(r) E(r) \tag{6}$$

It manipulates PBG in high speed but it cannot extract backward reflections and light wave propagation in the 2DPC structure. Hence, Maxwell's equation is employed in the time domain called FDTD method to analyse the field distribution of PC based

optical devices. FDTD method is employed to analyse the performance of transmission spectra of PC based optical devices. It simulates the electromagnetic devices for all range of frequencies from the microwave to the optical regime. It is one of the most important computational techniques for analysing the electromagnetic waves propagating through PC devices and for extracting backward reflections. It is a simple, attractive, accurate and efficient way to discretize Maxwell's equations. In this proposed structure, the normalized transmission spectra are obtained by taking fast Fourier transform (FFT) of the fields that are calculated by 2D FDTD method. Generally, 1D FDTD method offers fast simulation with less accuracy and 3D FDTD method requires more simulation time, large memory size and provides accurate behaviour of PCs. Even though 3D FDTD method affords accurate results, the same results can be obtained using 2D FDTD with less time and less memory space. Hence, 2D FDTD method is considered in the present work. In 2DPC, electromagnetic fields are propagated in the form of transversely two polarized modes (Eqs. (1) and (3)) TE and TM. The time stepping equation [40] for FDTD is given as follows:

$$E_x\Big|_{i,\,j}^{n+1} = E_x\Big|_{i,\,j}^{n} + \frac{c\Delta t}{\varepsilon_0}\,\frac{H_z\Big|_{i,\,j+1/2}^{n+1/2} - H_z\Big|_{i,\,j-1/2}^{n+1/2}}{\Delta y} \tag{7}$$

$$E_y\Big|_{i,\,j}^{n+1} = E_y\Big|_{i,\,j}^{n} - \frac{c\Delta t}{\varepsilon_0}\,\frac{H_z\Big|_{i+1/2,\,j}^{n+1/2} - H_z\Big|_{i-1/2,\,j}^{n+1/2}}{\Delta x} \tag{8}$$

$$H_z\Big|_{i,\,j}^{n+1/2} = E_z\Big|_{i,\,j}^{n-1/2} + \frac{c\Delta t}{\varepsilon_0}\left[\frac{E_x\Big|_{i,\,j+1/2}^{n} - E_x\Big|_{i,\,j-1/2}^{n}}{\Delta y} - \frac{E_y\Big|_{i+1/2,\,j}^{n} - E_y\Big|_{i-1/2,\,j}^{n}}{\Delta x}\right]$$

$$\tag{9}$$

where the indices *i* and *j* denote the discretized grid point in the *XY* plane and index *n* denotes the discrete time step.

3. Structural design

Figure 1 depicts a band diagram of the proposed structure before introducing the defects.

The structure is composed of Si rods embedded in air. The lattice constant *a* and radius *r* of the rods are 560 and 100 nm, respectively. The band diagram in Fig. 1 is calculated for the first Brillouin zone where the *x* axis is *Γ-X-M-Γ* which is called a wavevector or propagation constant. And the *x* axis is the point of the first Brillouin zone. The band diagram has two TE modes, where the electric field travels parallel to the rod axis and magnetic field travels perpendicular to the rod axis. The first and second TE PBG lie between $0.30233 < a/\lambda < 0.44593$ and $0.74448 < a/\lambda < 0.75959$, re-
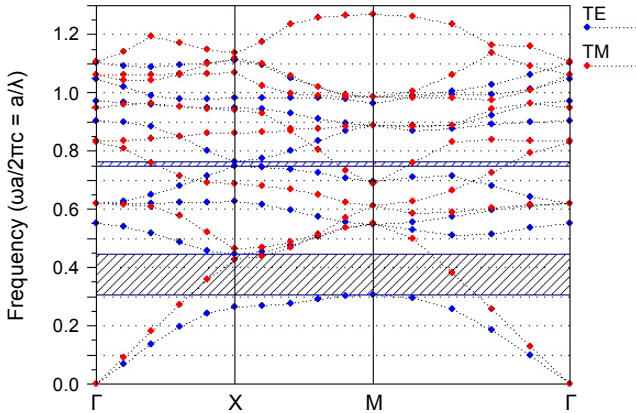
Fig. 1. Schematic representation of band diagram before introducing defects.

spectively. The wavelength range of first TE PBG is between 1255 to 1852 nm, which is considered in this work.

4. PCRR based eight channel demultiplexer

The proposed eight channel demultiplexer is shown in Fig. 2. It is composed of 40×60 periodic array of dielectric rods immersed in the air medium.
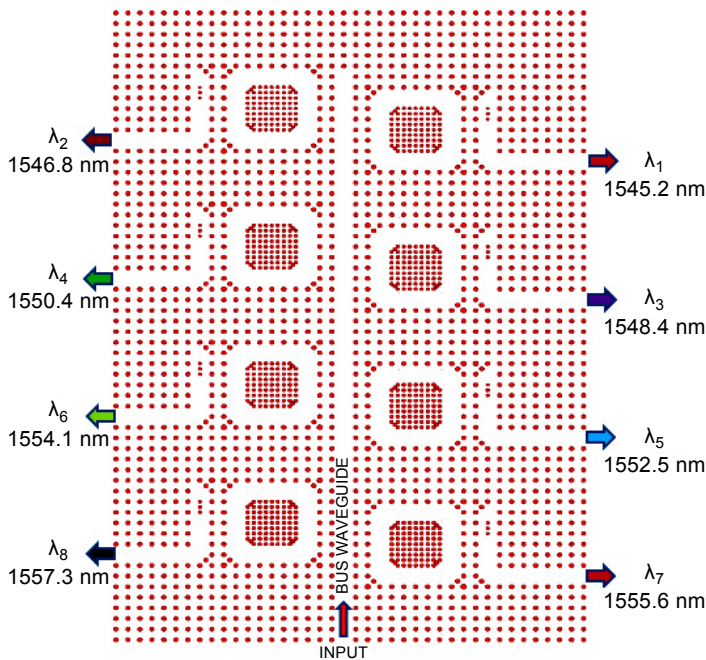

Fig. 2. Schematic representation of proposed PCRR based eight channel demultiplexer using MOC.

The proposed demulitplexer consists of eight octagonal ring resonators, bus waveguide and eight *L* bend waveguides. The octagonal ring resonator is used to select the desired channel whereas the *L* bend waveguide is employed for dropping the selected channel. The Gaussian light source is launched at the bottom end of the structure through a bus waveguide. The size of the bus waveguide is 920 nm ($2a$), which is useful to propagate the light waves linearly and distribute them to RRs through CRs. The footprint of the proposed structure is 752.64 μm^2. The output ports which are positioned in the right side from the bus waveguide of the PC structure are used to select odd numbers (λ_1, λ_3, λ_5 and λ_7) and ports in the left side are employed to drop even numbers (λ_2, λ_4, λ_6 and λ_8), which results in producing channels with low crosstalk. The proposed single channel demultiplexer (see Fig. 2) is composed of modified octagonal ring resonator, scatterer rods, coupling rods, channels selector rods and *L* bend waveguides.

The arrangement of the above mentioned rods is given below. The sectional view of a single RR of the proposed structure is depicted in Fig. 3**a** which comprises a ring resonator and *L* bend waveguide. The RR consists of a modified octagonal shaped cavity, scatterer rods and coupling rods. The *L* bend waveguide has channel selector rods to select the desired channel.

Modified octagonal cavity (MOC). It is constructed by varying the position of the inner rods and the period between the rods $0.28a$ (*i.e.*, $a/2$) as shown in Fig. 3**b**.
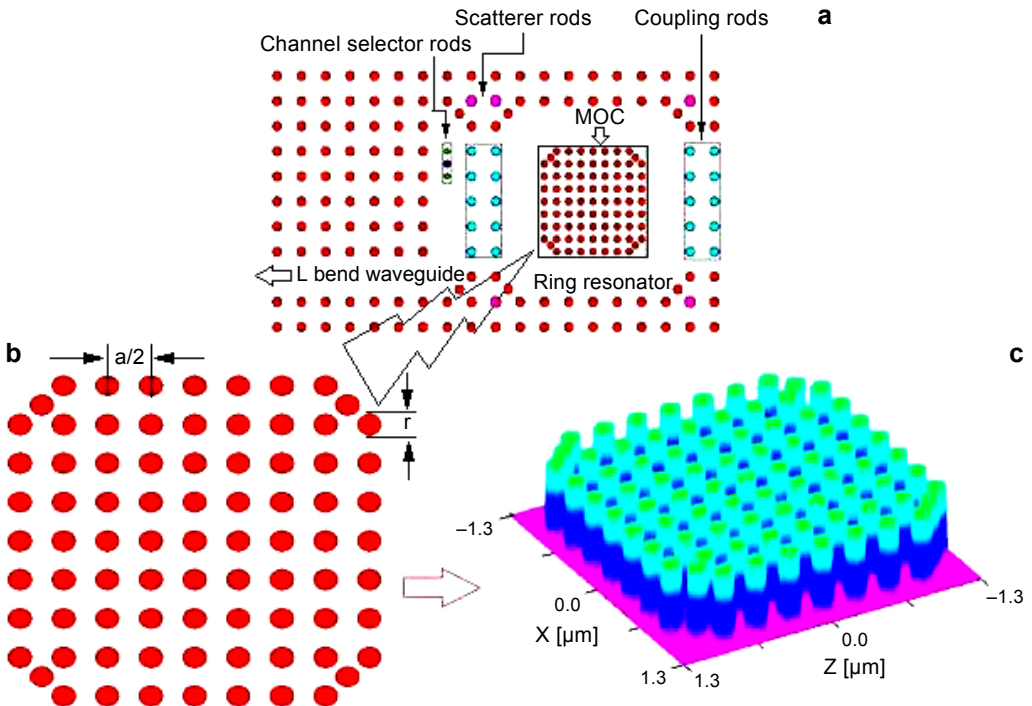

Fig. 3. Sectional view of single square MOC ring resonator (**a**), MOC (**b**), and 3D view of MOC (**c**).

T a b l e 1. Inner rod sizes in MOC with resonant wavelength of proposed eight channel demultiplexer.

Channel	Inner rod radius of MOC $r/2$ [nm]	Resonant wavelength λ_0 [nm]
λ_1	73	1545.2
λ_2	75	1546.8
λ_3	77	1548.4
λ_4	79	1550.4
λ_5	81	1552.5
λ_6	83	1554.1
λ_7	85	1555.6
λ_8	87	1557.3

The size of the MOC and its designated wavelength are given in Table 1. The radius of the rods in MOC is increased by 2 nm for every channel. From the Fig. 3**c**, the overall size of each MOC is about 6.76 μm^2. Hence, the average value of channel spacing is 1.7 nm. MOC is useful to control light within a narrow wavelength range and to make a narrow-bandwidth filter.

Scatterer rods (SRs). It is located at the corner of each RR and its size is 120 nm. The role of these rods is to suppress the counter propagation modes and to improve the spectral selectivity of the channel.

Coupling rods (CRs). The two columns of coupling rods (CRs) are located in-between MOC, bus waveguide and *L* bend dropping waveguide. The CRs are used to couple the propagation of light waves from bus waveguide to RR and RR to *L* bend waveguide. The size of each CR is 100 nm.

L bend waveguide. It is constructed by removing the rods in *L* shape. It drops the selected channels from RR. The channel selection part consists of three channel selector rods, which are located inside the *L* bend waveguide. It supports with MOC the selecting of the desired wavelength and improves the dropping efficiency. The radius of the centre rod in the channel selector is kept a 74 nm as constant for all the channels. However, the radius of the top and bottom rods in the channel selector is varied from 60 to 74 nm with 2 nm step (*i.e.*, 60 nm for λ_1, 62 nm for λ_2 and so on).

5. Simulation results and discussion

The signal is launched at the input port. The normalized transmission spectra are obtained at ports B, C and D by conducting FFT of the fields that are calculated by 2D FDTD method. The input and output signal power is recorded by power monitors which are positioned at the input and output ports. The normalized transmission is calculated through the following formula:

$$T(f) = \frac{1/2 \int \mathrm{Re}[\,p^{\mathrm{monitor}}(f)\,]\mathrm{d}S}{\text{Source power}} \qquad (10)$$

where $T(f)$ is a normalized transmission as a function of frequency, $p^{\text{monitor}}(f)$ represents Poynting vector monitored by the power monitor at the output port of the device and dS is the surface normal. The further normalization at the output side does not affect the result because of the source power normalization. Finally, the $T(f)$ is converted as a function of wavelength. The perfect matched layer (PML) is placed on all sides of the structure as an absorbing boundary condition to avoid the reflections in the computational domain. The reliability of the following numerical solution is ensured by the time steps Δt for electromagnetic fields propagating in 2DPC structure accurately

$$\Delta t \leq \frac{1}{c\sqrt{1/\Delta x^2 + 1/\Delta z^2}} \tag{11}$$

The excitation of TE polarized light is propagated in light velocity c along with XZ direction and its spatial steps are Δx and Δz. The grid sizes (Δx and Δz) are selected to be $a/16$ which equals 35 nm and the estimated FDTD time step Δt is 0.0175. If delta/16 is increased, it is highly possible to get the most precise output; however, it takes much time to get the desired response. If delta/16 is decreased, it is very difficult to predict the accurate behaviour of the proposed device. However, delta/16 is considered in this work as it offers the desired output with less computational time. The PML as an absorbing boundary condition is used to minimize the signal reflected from the launch field. The width of PML is 500 nm.

Figure 4 shows the normalized output spectrum of the proposed eight channel demultiplexer. The resonant wavelength of the eight channels is 1545.2 nm (λ_1), 1546.8 nm (λ_2), 1548.4 nm (λ_3), 1550.4 nm (λ_4), 1552.5 nm (λ_5), 1554.1 nm (λ_6), 1555.6 nm (λ_7) and 1557.3 nm (λ_8). The resonant wavelength, transmission efficiency,
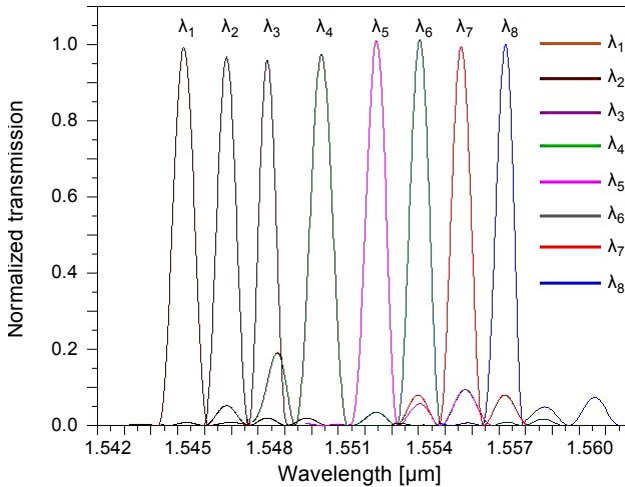

Fig. 4. Normalized output spectrum of proposed eight channel demultiplexer.

T a b l e 2. Resonant wavelength, spectral width, line spacing, transmission efficiency and quality factor of proposed eight channel demultiplexer.

Channel	Resonant wavelength λ_0 [nm]	Spectral width $\Delta\lambda$ [nm]	Line spacing [nm]	Transmission efficiency [%]	Quality factor Q
λ_1	1545.2	0.9	1.6	99	1545
λ_2	1546.8	0.8	1.6	96	1933
λ_3	1548.4	0.7	2.0	95	2212
λ_4	1550.4	0.9	2.1	98	1723
λ_5	1552.5	0.8	1.6	100	1941
λ_6	1554.1	0.7	1.5	100	2220
λ_7	1555.6	0.8	1.7	99	1945
λ_8	1557.3	0.7	1.7	100	2225

Q factor and spectral width of the channel 1 (λ_1) are 1545.2 nm, 99%, 1545 and 0.9 nm, respectively. The channel spacing is attained at 1.6 nm. The aforementioned functional characteristics of other channels λ_2–λ_8 are listed in Table 2.

Table 2 presents the resonant wavelength of eight channels (λ_1 to λ_8) along with spectral width, line spacing, transmission efficiency and Q factor. The spectral width $\Delta\lambda$ has been estimated by the Gaussian distribution function for a full width at half maximum (FWHM) of spectrum.

The electric field distribution of the proposed eight channel demultiplexer at $\lambda_7 = 1555.6$ nm is shown in Fig. 5. From the figure, it is observed that at ON resonance of port 7, the signals are transferred from the bus waveguide in the RR which in turn RR to output port 7. However, at OFF resonance, the signal is reflected back to the source without entering into the resonator. Based on the size of the modified octagonal RR,
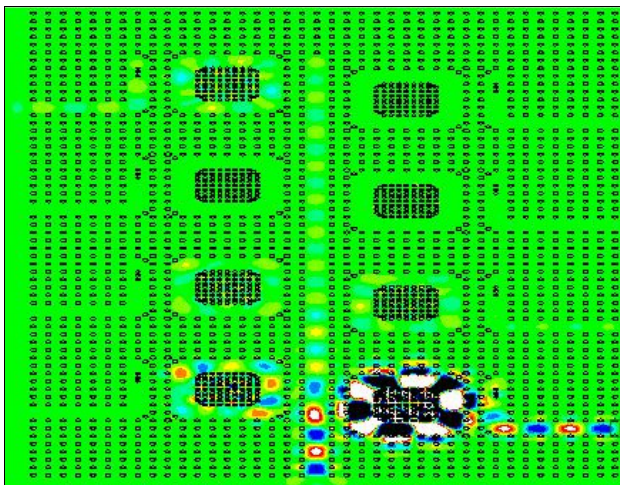

Fig. 5. Field distribution of channel λ_7 (1555.6 nm) for proposed eight channel demultiplexer.

T a b l e   3. Crosstalk of proposed eight channels demultiplexer.

X_{ij} [dB]	λ_1	λ_2	λ_3	λ_4	λ_5	λ_6	λ_7	λ_8
λ_1	·	−26.8	·	·	·	·	·	·
λ_2	−26.9	·	−29.8	·	·	·	·	·
λ_3	·	−29.8	·	−29.9	·	·	·	·
λ_4	·	·	−29.7	·	−30.0	·	·	·
λ_5	·	·	·	−29.9	·	−20.9	·	·
λ_6	·	·	·	·	−20.9	·	−22.9	·
λ_7	·	·	·	·	·	−20.4	·	−27.0
λ_8	·	·	·	·	·	·	−26.9	·

the appropriate wavelength is selected and passed on to the concerned dropping *L* bend waveguide.

Table 3 shows the crosstalk between the channels. The crosstalk X_{ij} of channels i and j varies from 1 to 8. It shows the crosstalk of channel i at the resonant wavelength of channel j as well as the crosstalk of channel j at the resonant wavelength channel i. The minimum value of the crosstalk is –30 dB which facilitates better performance of the demultiplexer. In addition, the channel selector rods and MOC play a role in diminishing the crosstalk. It is noticed that the proposed demultiplexer offers better channel spacing, Q factor, transmission efficiency and crosstalk than the reported one. Besides that, the present work covers the third window of optical communication.

6. Conclusion

In this paper, 2DPC based eight channels demultiplexer is proposed and designed using an octagonal ring resonator for WDM applications. The functional parameters, namely resonant wavelength, Q factor, channel spacing, spectral width, output efficiency and crosstalk are investigated. In this attempt, the channel selection is carried out by altering the size of the octagonal ring resonator. The average transmission efficiency, Q factor, spectral width and channel spacing of the proposed demultiplexer are 98%, 1968, 0.8 nm and 1.7 nm, respectively. The crosstalk of the proposed demultiplexer is very low and amounts to –30 dB as the even number of channels and the odd number of channels are dropped separately. The size of the demultiplexer is about 752.64 μm^2. The functional characteristics of the proposed demultiplexer are meeting the requirements of WDM systems, hence this demultiplexer can be incorporated for integrated optics.

References

[1] Keiser G.E., *A review of WDM technology and applications*, Optical Fiber Technology **5**(1), 1999, pp. 3–39.
[2] Jie Zha, Zhi-Yong Zhong, Huai-Wu Zhang, Qi-Ye Wen, *Differences of band gap characteristics of square and triangular lattice photonic crystals in terahertz range*, Journal of Electronic Science and Technology **7**(3), 2009, pp. 268–271.

[3] PARTHA SONA MAJI, PARTHA ROY CHAUDHURI, *Near-elliptic core triangular-lattice and square-lattice PCFs: a comparison of birefringence, cut-off and GVD characteristics towards fiber device application*, Journal of the Optical Society of Korea **18**(3), 2014, pp. 207–216.

[4] JOANNOPOULOS J.D., MEADE R.D., WINN J.N., *Photonic Crystals: Molding the Flow of Light*, Princeton University Press, Princeton, NI, USA, 1995.

[5] ROBINSON S., NAKKEERAN R., *Bandstop filter for photonic integrated circuits using photonic crystal with circular ring resonator*, Journal of Nanophotonics **5**(1), 2011, article ID 053521.

[6] ROBINSON S., NAKKEERAN R., *Performance evaluation of add drop filter by studying rod shape and filling fraction*, Optoelectronics and Advanced Materials: Rapid Communications **5**, 2011, pp. 948–955.

[7] ROBINSON S., NAKKEERAN R., *Investigation on two dimensional photonic crystal resonant cavity based bandpass filter*, Optik – International Journal for Light and Electron Optics **123**(5), 2012, pp. 451–457.

[8] HAMED ALIPOUR-BANAEI, FARHAD MEHDIZADEH, *Significant role of photonic crystal resonant cavities in WDM and DWDM communication tunable filters*, Optik – International Journal for Light and Electron Optics **124**(17), 2013, pp. 2639–2644.

[9] ZEXUAN QIANG, WEIDONG ZHOU, SOREF R.A., *Optical add-drop filters based on photonic crystal ring resonators*, Optics Express **15**(4), 2007, pp. 1823–1831.

[10] ROBINSON S., NAKKEERAN R., *Photonic crystal ring resonator based add-drop filter using hexagonal rods for CWDM systems*, Optoelectronics Letters **7**(3), 2011, pp. 164–166.

[11] LI L., LIU G.Q., *Photonic crystal ring resonator channel drop filter*, Optik – International Journal for Light and Electron Optics **124**(17), 2013, pp. 2966–2968.

[12] TAALBI A., BASSOU G., MAHMOUD M.Y., *New design of channel drop filters based on photonic crystal ring resonators*, Optik – International Journal for Light and Electron Optics **124**(9), 2013, pp. 824–827.

[13] MAHMOUD YOUCEF MAHMOUD, GHAOUTI BASSOU, AHMED TAALBI, ZOHEIR MOHAMED CHEKROUN, *Optical channel drop filters based on photonic crystal ring resonators*, Optics Communications **285**(3), 2012, pp. 368–372.

[14] WENYUAN RAO, YANJUN SONG, MINGKAI LIU, CHONGJUN JIN, *All-optical switch based on photonic crystal microcavity with multi-resonant modes*, Optik – International Journal for Light and Electron Optics **121**(21), 2010, pp. 1934–1936.

[15] LIU Y., SALEMINK H.W.M., *Photonic crystal-based all-optical on-chip sensor*, Optics Express **20**(18), 2012, pp. 19912–19920.

[16] YONGHAO CUI, QI WU, SCHONBRUN E., TINKER M., LEE J.-B., WON PARK, *Silicon-based 2-D slab photonic crystal TM polarizer at telecommunication wavelength*, IEEE Photonics Technology Letters **20**(8), 2008, pp. 641–643.

[17] DAQUAN YANG, HUIPING TIAN, YUEFENG JI, *High-bandwidth and low-loss photonic crystal power-splitter with parallel output based on the integration of Y-junction and waveguide bends*, Optics Communications **285**(18), 2012, pp. 3752–3757.

[18] INSU PARK, HYUN-SHIK LEE, HYUN-JUN KIM, KYUNG-MI MOON, SEUNG-GOL LEE, BEOM-HOAN O, SE-GEUN PARK, EL-HANG LEE, *Photonic crystal power-splitter based on directional coupling*, Optics Express **12**(15), 2004, pp. 3599–3604.

[19] MANZACCA G., PACIOTTI D., MARCHESE A., SVALUTO MOREOLO M., CINCOTTI G., *2D photonic crystal cavity-based WDM multiplexer*, Photonics and Nanostructures – Fundamentals and Applications **5**(4), 2007, pp. 164–170.

[20] SWATI RAWAL, SINHA R.K., *Design, analysis and optimization of silicon-on-insulator photonic crystal dual band wavelength demultiplexer*, Optics Communications **282**(19), 2009, pp. 3889–3894.

[21] ROSTAMI A., NAZARI F., ALIPOUR BANAEI H., BAHRAMI A., *A novel proposal for DWDM demultiplexer design using modified-T photonic crystal structure*, Photonics and Nanostructures – Fundamentals and Applications **8**(1), 2010, pp. 14–22.

[22] ROSTAMI A., ALIPOUR BANAEI H., NAZARI F., BAHRAMI A., *An ultra-compact photonic crystal wavelength division demultiplexer using resonance cavities in a modified Y-branch structure*, Optik – International Journal for Light and Electron Optics **122**(16), 2011, pp. 1481–1485.

[23] Xuan Zhang, Qinghua Liao, Tianbao Yu, Nianhua Liu, Yongzhen Huang, *Novel ultracompact wavelength division demultiplexer based on photonic band gap*, Optics Communications **285**(3), 2012, pp. 274–276.

[24] Bouamami S., Naoum R., *Compact WDM demultiplexer for seven channels in photonic crystal*, Optik – International Journal for Light and Electron Optics **124**(16), 2013, pp. 2373–2375.

[25] Djavid M., Monifi F., Ghaffari A., Abrishamian M.S., *Heterostructure wavelength division demultiplexers using photonic crystal ring resonators*, Optics Communications **281**(15–16), 2008, pp. 4028–4032.

[26] Rakhshani M.R., Mansouri-Birjandi M.A., *Heterostructure four channel wavelength demultiplexer using square photonic crystals ring resonators*, Journal of Electromagnetic Waves and Applications **26**(13), 2012, pp. 1700–1707.

[27] Mansouri-Birjandi M.A., Rakhshani M.R., *A new design of tunable four port wavelength demultiplexer by photonic crystal ring resonators*, Optik – International Journal for Light and Electron Optics **124**(23), 2013, pp. 5923–5926.

[28] Ghorbanpour H., Makouei S., *2-channel all optical demultiplexer based on photonic crystal ring resonator*, Frontiers of Optoelectronics **6**(2), 2013, pp. 224–227.

[29] Rakhshani M.R., Mansouri-Birjandi M.A., *Design and simulation of wavelength demultiplexer based on heterostructure photonic crystals ring resonators*, Physica E: Low-dimensional Systems and Nanostructures **50**, 2013, pp. 97–101.

[30] Alipour-Banaei H., Farhad Mehdizadeh, Somaye Serajmohammadi, *A novel 4-channel demultiplexer based on photonic crystal ring resonators*, Optik – International Journal for Light and Electron Optics **124**(23), 2013, pp. 5964–5967.

[31] Nikhil Deep Gupta, Vijay Janyani, *Dense wavelength division Demultiplexing using photonic crystal waveguides based on cavity resonance*, Optik – International Journal for Light and Electron Optics **125**(19), 2014, pp. 5833–5836.

[32] Mehdizadeh F., Soroosh M., *A new proposal for eight-channel optical demultiplexer based on photonic crystal resonant cavities*, Photonic Network Communications **31**(1), 2016, pp. 65–70.

[33] Xiang-nan Zhang, Gui-qiang Liu, Zhengqi Liu, Ying Hu, Mulin Liu, *Three-channels wavelength division multiplexing based on asymmetrical coupling*, Optik – International Journal for Light and Electron Optics **126**(11–12), 2015, pp. 1138–1141.

[34] Alipour-Banaei H., Serajmohammadi S., Mehdizadeh F., *Optical wavelength demultiplexer based on photonic crystal ring resonators*, Photonic Network Communications **29**(2), 2015, pp. 146–150.

[35] Venkatachalam K., Sriram Kumar D., Robinson S., *Analysis and design of photonic crystal based demultiplexer*, 2015 3rd International Conference on Signal Processing, Communication and Networking (ICSCN), 2015, pp. 1–4.

[36] Johnson S.G., Joannopoulos J.D., *Block-iterative frequency-domain methods for Maxwell's equations in a planewave basis*, Optics Express **8**(3), 2001, pp. 173–190.

[37] Pendry J.B., MacKinnon A., *Calculation of photon dispersion relations*, Physical Review Letters **69**(19), 1992, pp. 2772–2775.

[38] Taflove A., Hegness S.C., *Computational Electrodynamics: The Finite-Difference Time-Domain Method*, 2nd Ed., Artech House, Boston, MA, USA, 2000.

[39] Pelosi G., Coccioli R., Selleri S., *Quick Finite Elements for Electromagnetic Waves*, Artech House, Boston, London, 1997.

[40] Kane Yee, *Numerical solution of initial boundary value problems involving Maxwell's equation in isotropic media*, IEEE Transactions on Antennas and Propagation **14**(3), 1996, pp. 302–307.